Dirac Fermions in Inhomogeneous Magnetic Field

Ahmed Jellal[a,b,c*] and **Abderrahim El Mouhafid**[c†]

[a] *Physics Department, College of Science, King Faisal University,*
PO Box 380, Alahsa 31982, Saudi Arabia
[b] *Saudi Center for Theoretical Physics, Dhahran, Saudi Arabia*
[c] *Theoretical Physics Group, Faculty of Sciences, Chouaïb Doukkali University,*
PO Box 20, 24000 El Jadida, Morocco

Abstract

We study a confined system of Dirac fermions in the presence of inhomogeneous magnetic field. Splitting the system into different regions, we determine their corresponding energy spectrum solutions. We underline their physical properties by considering the conservation energy where some interesting relations are obtained. These are used to discuss the reflexion and transmission coefficients for Dirac fermions and check the probability condition for different cases. We generalize the obtained results to a system with gap and make some analysis. After evaluating the current-carrying states, we analyze the Klein paradox and report interesting discussions.

*jellal@pks.mpg.de, ahjellal@kfu.edu.sa
†elmouhafid@gmail.com

1 Introduction

The Dirac formalism plies an important role not only from mathematical point of view but physical one as well. The recent observation of the anomalous quantum Hall effect in graphene [1, 2] renewed the interest to this formalism. In fact, many questions, raised in graphene, found their solutions by adopting the Dirac formalism as cornerstone. Among them, we cite the confinement [3] that is much needed to describe the transport properties in graphene. Subject that attracted much attention where interesting developments appeared by dealing with different issues, for instance we refer to [4, 5].

On the other hand, the quantum wires (electron waveguides) with quantized conductance can be formed in graphene [6]. Such electron waveguides are indispensable parts of any conceivable all-graphene device. In lithographically formed graphene ribbons, the electronic bandstructure is theoretically expected to very sensitively depend on the width and on details of the boundary [7]. On top of that, disorder and structural inhomogeneity are substantial in real graphene [8]. For narrow graphene ribbons or electrostatically formed graphene wires [9], conventional conductance quantization thus seems unlikely [10]. This expectation is in accordance with recent experiments [11].

Magnetic barrier technology is well developed [12, 13, 14] and its application to graphene samples appears to pose no fundamental problems [6]. In fact, snake states are experimentally studied in other materials [12, 15], mainly motivated by the quest for electrical rectification. On the theory side, the confined Schrödinger fermions in the magnetic field (with $B' = 0$) is discussed [16] as well as the asymmetric cases [17]. For the Dirac-Weyl quasiparticles encountered in graphene, however, such calculations are not reported. The inhomogeneous magnetic field case in graphene is analyzed in [18]. Theoretically, the electron waveguides, in graphene created by suitable inhomogeneous magnetic fields, is considered [6]. The properties of uni-directional snake states are discussed. For a certain magnetic field profile, two spatially separated counter-propagating snake states are formed, leading to conductance quantization insensitive to backscattering by impurities or irregularities of the magnetic field.

Subsequently, The tunneling effect of two-dimensional Dirac fermions in a constant magnetic field is studied [19]. This is done by using the continuity equation at fixed points to determine the corresponding reflexion and transmission coefficients. For this, a system made of graphene, as superposition of two different regions where the second is characterized by an energy gap t', is considered. In fact, concrete systems are treated to practically give two illustrations: barrier and diode. For each case, the transmission in terms of the ratio of the energy conservation and t' are discussed. Moreover, the resonant tunneling by introducing a scalar Lorentz potential is analyzed where it is shown that a total transmission is possible.

Motivated by the above progress and in particular [6, 19], we deal with other features of the system considered in [6]. Such system is composed of different regions submitted to two magnetic fields and confined to a constant potential. This allows us to treat each region separately by determining the corresponding energy spectrum solutions. We underline some physical properties of their spectrum by taking into account of the energy conservation where interesting relations are obtained. Using the continuity at different points, we explicitly evaluate the reflexion and transmission coefficients. Combining all, we chow that the probability condition is well verified. As second task, we consider the present system with energy gap t' and do the same job to derive its eigenspinors as well as eigenvalues.

It is shown that even the reflexion and transmission coefficients take new forms in terms of gap but the probability condition still verified. Interesting limits are discussed, which concern total reflexion and transmission of the system with gap.

Finally, we treat the Klein paradox by using the current-carrying states where different limits and discussions are presented. More precisely, we evaluate the currents for each region and use their relations to the reflexion and transmission coefficients to check the probabilities. Subsequently, three different cases are considered, which correspond to week, intermediate and strong potentials. We notice that two last cases are shown negative transmissions. However, by combining all coefficients we end up with a sum equal unity.

The present paper is organized as follows. In section 2, we consider a confined Dirac fermion in inhomogeneous magnetic field (1). After getting the eigenvalues and eigenfunctions, we analyze the energy conservation that allows us to derive interesting relations between involved quantum numbers and parameters. In section 3, we study scattering between two regions to determine the reflexion and transmission coefficients, which will be used to discuss the probability conditions of the present system. We do the same job in section 4 but by considering three regions where the first is equivalent to the third. The continuity at each point leads to express the coefficients entering in the game in terms of different parameters. In section 5, we introduce a gap like a mass term and analyze the tunneling effect of such case. We study the Klein paradox in section 6 by involving the currents corresponding to different regions and consider three cases. Finally, we close by concluding our work.

2 Dirac fermions in inhomogeneous magnetic field

We consider a system of massless Dirac fermions through a strip of graphene characterized by the length d and width W in the presence of inhomogeneous magnetic field. More precisely, we introduce two magnetic fields B and B', such as

$$B(x) = \begin{cases} B, & x < -d \\ B', & |x| < d \\ B, & x > d. \end{cases} \tag{1}$$

According to the configuration (1), we decompose the present system into three regions. Schematically, we end up with Figure 1

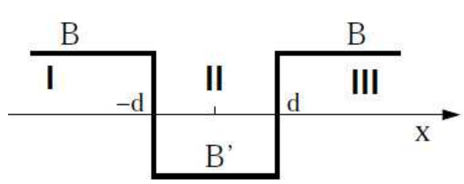

Figure 1: Magnetic field profile.

Clearly, regions I and III are similar but different with respect to region II. Note that, the system characterized by Figure 1 has been analyzed in [6] for possible quantum wires in graphene. However, in the present work we study other features of such system to deal with different issues, which concern tunneling effect and Klein paradox.

2.1 Dirac Hamiltonian

Before writing down the appropriate Hamiltonian of the system (Figure 1), let us derive the corresponding gauge field to the configuration (1). Indeed, using the continuity of the potential to obtain

$$A_{\mathsf{j}}(x) = \begin{cases} A_{\mathsf{I}}(x) = Bx + (B - B')d, & x < -d \\ A_{\mathsf{II}}(x) = B'x, & |x| < d \\ A_{\mathsf{III}}(x) = Bx - (B - B')d, & x > d. \end{cases} \tag{2}$$

where j is labeling regions I, II and III . It clear that, for $B = B'$ we end up with one potential and therefore three regions become similar to each others.

In the systems made of graphene, the two Fermi points, each with a two-fold band degeneracy, can be described by a low-energy continuum approximation with a four-component envelope wavefunction whose components are labeled by a Fermi-point pseudospin $= \pm 1$ and a sublattice forming an honeycomb. Specifically, the Hamiltonian for one-pseudospin component for the present system can be written as

$$H_{\mathsf{j}} = \upsilon_F \vec{\sigma} \cdot \vec{\pi}_{\mathsf{j}} + V_{\mathsf{j}}(x) \tag{3}$$

where the components of the conjugate momentum $\vec{\pi}_{\mathsf{j}} = \vec{p} + \frac{e}{c}\vec{A}_{\mathsf{j}}$ are given by

$$\pi_{x,\mathsf{j}} = p_x, \qquad \pi_{y,\mathsf{j}} = p_y + \frac{e}{c} A_{\mathsf{j}}(x) \tag{4}$$

and $V_{\mathsf{j}}(x)$ is the potential barrier that has a rectangular shape, which is infinite along the y-axis and has the form

$$V_{\mathsf{j}}(x) = \begin{cases} V_0, & -d < x < d \\ 0, & \text{otherwise} \end{cases} \tag{5}$$

where $V_0 > 0$. Injecting all in (3) to get

$$H_{\mathsf{j}} = \upsilon_F \begin{pmatrix} V_{\mathsf{j}}(x)/\upsilon_F & p_x - ip_y - i\frac{e}{c}A_{\mathsf{j}}(x) \\ p_x + ip_y + i\frac{e}{c}A_{\mathsf{j}}(x) & V_{\mathsf{j}}(x)/\upsilon_F \end{pmatrix}. \tag{6}$$

At this stage, it is convenient to introduce the annihilation and creation operators. They can be defined as

$$a_{\mathsf{j}} = ip_x + p_y + \frac{e}{c} A_{\mathsf{j}}(x), \qquad a_{\mathsf{j}}^{\dagger} = -ip_x + p_y + \frac{e}{c} A_{\mathsf{j}}(x) \tag{7}$$

which obey the canonical commutation relations

$$\left[a_{\mathsf{j}}, a_{\mathsf{j}}^{\dagger}\right] = \begin{cases} \frac{2\hbar^2}{l_B^2}, & j = \mathsf{I} \\ \frac{2\hbar^2}{l_{|B'|}^2}, & j = \mathsf{II} \\ \frac{2\hbar^2}{l_B^2}, & j = \mathsf{III} \end{cases} \tag{8}$$

where the magnetic lengths $l_B = \sqrt{\frac{\hbar c}{eB}}$ and $l_{|B'|} = \sqrt{\frac{\hbar c}{e|B'|}}$ are corresponding to the magnetic fields B and B', respectively. The Hamiltonian (6) can be written in terms of a_{j} and $a_{\mathsf{j}}^{\dagger}$ as

$$H_{\mathsf{j}} = i\upsilon_F \begin{pmatrix} V_{\mathsf{j}}(x)/i\upsilon_F & -a_{\mathsf{j}} \\ a_{\mathsf{j}}^{\dagger} & V_{\mathsf{j}}(x)/i\upsilon_F \end{pmatrix} \tag{9}$$

which is encoding all regions. This will be used to study each region separately and derive the corresponding energy spectrum solutions.

2.2 Energy spectrum solutions

We determine the eigenvalues and eigenspinors of the Hamiltonian H_{j}. Indeed, the the Dirac Hamiltonian describing region I is obtained from (9) as

$$H_{\mathsf{I}} = iv_F \begin{pmatrix} 0 & -a_{\mathsf{I}} \\ a_{\mathsf{I}}^{\dagger} & 0 \end{pmatrix}. \tag{10}$$

The operators a_{I} and $a_{\mathsf{I}}^{\dagger}$ can be rescaled to define others, such as

$$b_{\mathsf{I}} = \frac{l_B}{\sqrt{2}\hbar} a_{\mathsf{I}}, \qquad b_{\mathsf{I}}^{\dagger} = \frac{l_B}{\sqrt{2}\hbar} a_{\mathsf{I}}^{\dagger} \tag{11}$$

which verify

$$[b_{\mathsf{I}}, b_{\mathsf{I}}^{\dagger}] = \mathbb{I}. \tag{12}$$

Using these to write H_{I} as

$$H_{\mathsf{I}} = i\hbar\omega_c \begin{pmatrix} 0 & -b_{\mathsf{I}} \\ b_{\mathsf{I}}^{\dagger} & 0 \end{pmatrix} \tag{13}$$

where we have set $\omega_c = \sqrt{2}\frac{v_F}{l_B}$ as a cyclotron frequency.

To get the energy spectrum solutions of (13), we solve the eigenvalue equation for a given spinor $\phi_{\mathsf{I}} = \begin{pmatrix} \varphi_1 \\ \varphi_2 \end{pmatrix}$ of H_{I}. This is

$$H_I \begin{pmatrix} \varphi_1 \\ \varphi_2 \end{pmatrix} = E_{\mathsf{I}} \begin{pmatrix} \varphi_1 \\ \varphi_2 \end{pmatrix} \tag{14}$$

which is equivalent to

$$i\hbar\omega_c \begin{pmatrix} 0 & -b_{\mathsf{I}} \\ b_{\mathsf{I}}^{\dagger} & 0 \end{pmatrix} \begin{pmatrix} \varphi_1 \\ \varphi_2 \end{pmatrix} = E_{\mathsf{I}} \begin{pmatrix} \varphi_1 \\ \varphi_2 \end{pmatrix} \tag{15}$$

and leads to two relations between spinor components

$$-i\hbar\omega_c b_{\mathsf{I}} \varphi_2 = E_{\mathsf{I}} \varphi_1 \tag{16}$$

$$i\hbar\omega_c b_{\mathsf{I}}^{\dagger} \varphi_1 = E_{\mathsf{I}} \varphi_2. \tag{17}$$

Now inserting (16) into (17) to obtain a differential equation of second order for φ_2

$$\hbar^2\omega_c^2 b_{\mathsf{I}}^{\dagger} b_{\mathsf{I}} \varphi_2 = E_{\mathsf{I}}^2 \varphi_2. \tag{18}$$

It is clear that φ_2 is an eigenstate of the number operator $\hat{n} = b_{\mathsf{I}}^{\dagger} b_{\mathsf{I}}$ and therefore we identify φ_2 to the eigenstates of the harmonic oscillator $\mid n\rangle$, namely

$$\varphi_2 \sim \mid n\rangle \tag{19}$$

and its eigenvalues read as

$$E_{\mathsf{I},n} = s\hbar\omega_c \sqrt{|n|} \tag{20}$$

where n is obviously the eigenvalues of $\hat{n}$, with $n = 0, \pm1, \pm2, \cdots$, and $s = \mathsf{sgn}(n)$. Note that, $n = 0$ corresponds to the lowest Landau level, i.e. zero mode energy.

Using (16), (19) and (20) to get the first component as

$$\varphi_1 = \frac{-i\hbar\omega_c}{E_{\mathsf{I}}} b_{\mathsf{I}} \mid n\rangle = -is \mid n-1\rangle \tag{21}$$

which gives the eigenspinors

$$\phi_{\mathsf{I},n} \sim \begin{pmatrix} -si \mid n-1\rangle \\ \mid n\rangle \end{pmatrix}. \tag{22}$$

In terms of the parabolic cylinder functions $D_n(x + x_{01})$ [20], the eigenspinors in the plane (x, y) are

$$\phi_{\mathsf{I},n,k_y}(x,y) = \frac{1}{\sqrt{2}} \begin{pmatrix} -siD_{|n|-1}(x + x_{01}) \\ D_{|n|}(x + x_{01}) \end{pmatrix} e^{ik_y y} \tag{23}$$

where $x_{01} = k_y l_B^2 + \left(1 - \frac{|B'|}{B}\right) d$ and $D_n(x)$ are related to Hermite polynomials via

$$D_n(x) = \left(l_B\sqrt{\pi} n! 2^n\right)^{-\frac{1}{2}} \exp\left(-\frac{x^2}{2}\right) H_n(x). \tag{24}$$

As far as region II is concerned, we use the mapping $n \longrightarrow m$ and $s \longrightarrow s'$ in (23) to obtain the eigenspinors $\phi_{\mathsf{II},m,k_y}(x,y)$ in terms of $x_{02} = q_y l_{|B'|}^2$ and the corresponding eigenvalues

$$E_{\mathsf{II},m} = s'\hbar\omega_c'\sqrt{|m|} + V_0 \tag{25}$$

where $s' = \mathsf{sgn}(m)$ and $\omega_c' = \sqrt{2}\frac{v_F}{l_{|B'|}}$ is the cyclotron frequency associated to the magnetic field B'.

Finally, for region III the eigenvalues and the eigenspinors are similar to those of region I except that the correspondence

$$x_{01} \longrightarrow x_{03} = k_y l_B^2 - \left(1 - \frac{|B'|}{B}\right) d \tag{26}$$

must be taken into account in (23). Note that, for $B' = -B$ (with $B' < 0$) the eigenspinors for three regions can be expressed with the same position $x_0 = k_y l_B^2$.

2.3 Illustrations

To give some illustrations, we focus on the eigenfunctions of four lowest states in region II, which are summarized in Table 1. Different plots are given in Figure 2 those show that the m^{th} eigenfunction has m-nodes, namely there are m-values of x for which $\phi_{\mathsf{II},m}(x) = 0$.

Number	Energy eigenvalue	Energy eigenfunction
$m = 0$	$E_{\mathsf{II},0} = V_0$	$\phi_{\mathsf{II},0}(x) = \left(\frac{1}{l_{\|B'\|}\sqrt{\pi}}\right)^{\frac{1}{2}} e^{-(x+x_{02})^2/2l_{\|B'\|}^2}$
$m = 1$	$E_{\mathsf{II},1} = \hbar\omega_c' + V_0$	$\phi_{\mathsf{II},1}(x) = \left(\frac{1}{2l_{\|B'\|}\sqrt{\pi}}\right)^{\frac{1}{2}} 2\left(\frac{x+x_{02}}{l_{\|B'\|}}\right) e^{-(x+x_{02})^2/2l_{\|B'\|}^2}$
$m = 2$	$E_{\mathsf{II},2} = \sqrt{2}\hbar\omega_c' + V_0$	$\phi_{\mathsf{II},2}(x) = \left(\frac{1}{8l_{\|B'\|}\sqrt{\pi}}\right)^{\frac{1}{2}} \left[4\left(\frac{x+x_{02}}{l_{\|B'\|}}\right)^2 - 2\right] e^{-(x+x_{02})^2/2l_{\|B'\|}^2}$
$m = 3$	$E_{\mathsf{II},3} = \sqrt{3}\hbar\omega_c' + V_0$	$\phi_{\mathsf{II},3}(x) = \left(\frac{1}{48l_{\|B'\|}\sqrt{\pi}}\right)^{\frac{1}{2}} \left[8\left(\frac{x+x_{02}}{l_{\|B'\|}}\right)^3 - 12\left(\frac{x+x_{02}}{l_{\|B'\|}}\right)\right] e^{-(x+x_{02})^2/2l_{\|B'\|}^2}$

Table 1: Normalized eigenfunctions for four lowest states of a one-dimensional potential energy field.

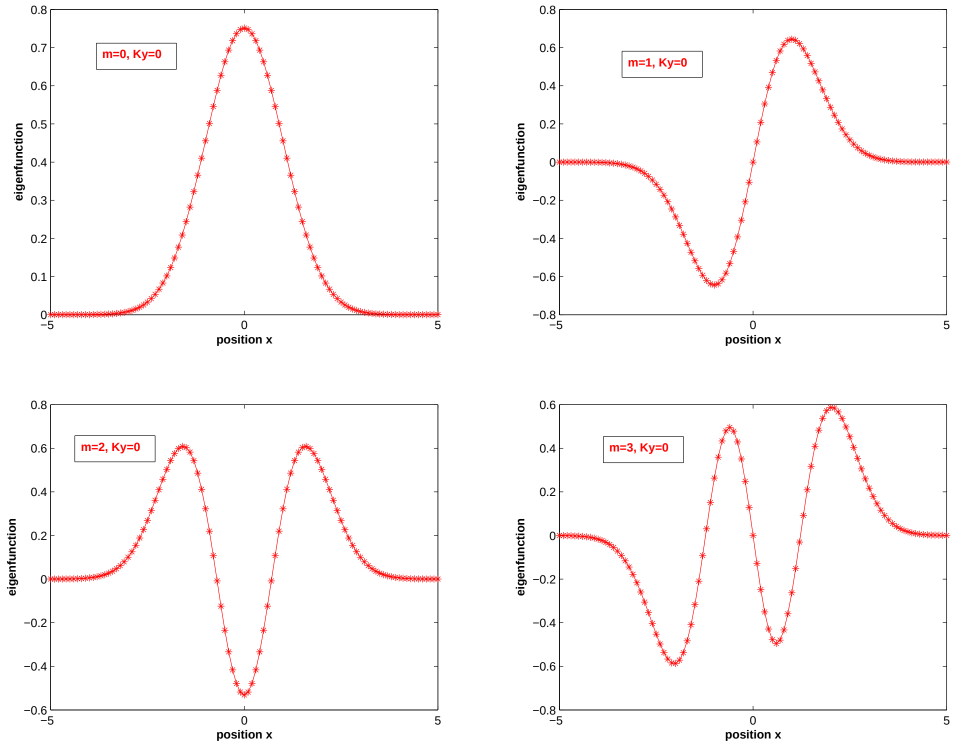

Figure 2: The spatial shapes of the eigenfunctions $\phi_{\text{II},m}(x)$, with $m = 0, 1, 2, 3$ and $l_{|B'|} = \sqrt{\frac{\hbar c}{e|B'|}} = 1$.

On the other hand, the wavefunctions have observable properties. Indeed, if the position coordinate is changed from x to -x, the eigenfunction has a definite symmetry

$$\begin{cases} \phi_{\text{II},m}(-x) = +\phi_{\text{II},m}(x), & \text{if } m \text{ is even} \\ \phi_{\text{II},m}(-x) = -\phi_{\text{II},m}(x), & \text{if } m \text{ is odd} \end{cases} \tag{27}$$

which is nothing but the parity symmetry. Furthermore, the position probability density of fermion is given by

$$|\phi_m(x, y)|^2 = |\phi_m(x)|^2. \tag{28}$$

By plotting this for some specific values of m, we deduce an interesting conclusion. From Figure 3, we notice that the fermion can have any location between $x = -\infty$ and $x = +\infty$, in marked contrast with a classical fermion, which is confined to the region $-A < x < +A$ where A is the amplitude of oscillation.

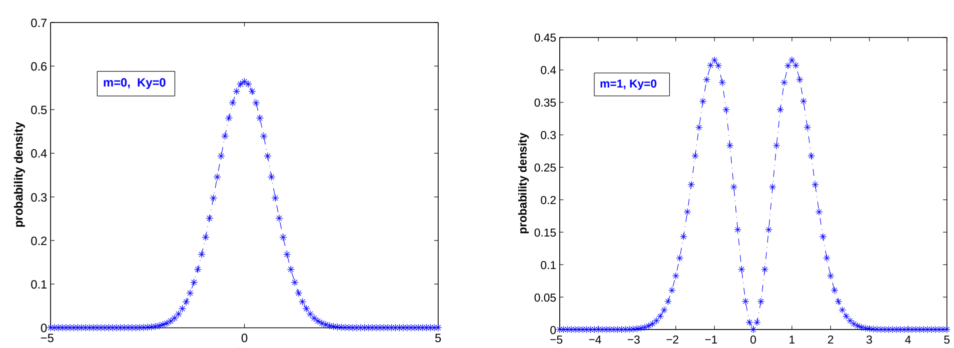

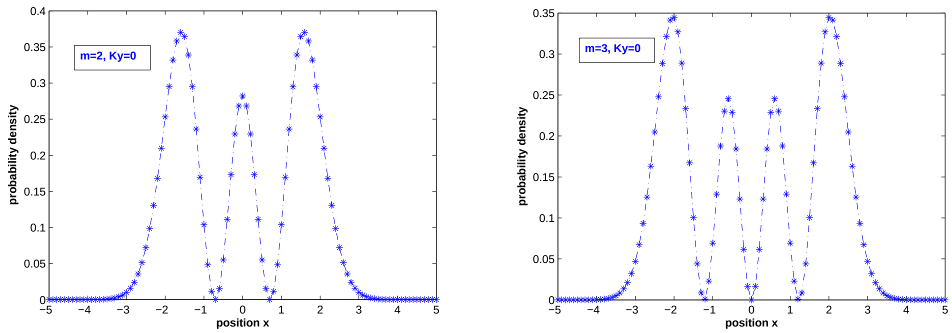

Figure 3: The position probability densities $|\phi_{\mathrm{II},m}(x)|^2$ corresponding to Table 1.

2.4 Energy conservation

In the interface between regions, there is conservation of the tangent components of the wave vector, i.e. $k_y = q_y$, and conservation of the energy. This is

$$E_{\mathrm{I}} = E_{\mathrm{II}} = E \tag{29}$$

which leads to the constraint

$$\frac{|n|}{|m|} = \frac{|B'|}{B} \frac{E^2}{(E - V_0)^2}. \tag{30}$$

Since n and m are integer values, the r.h.s term must be a fractional number, which can be written as

$$|n| = K\ |m|, \qquad K \in \mathbb{Q}^+. \tag{31}$$

This relation is very important because without such set one can not talk about tunneling effect in the present case. We will clarify this statement from next section and exactly when we begin by calculating different quantities in order to check the probability condition.

Now let us return to (20) and (25) to write the ratio as

$$\frac{E}{V_0} = \frac{\sqrt{|n|}}{\sqrt{|n|} - \frac{s'}{s}\sqrt{\frac{|B'|}{B}|m|}}. \tag{32}$$

Recall that in the region II we have $V_0 > 0$, which implies that the energy E can be either positive or negative. Therefore, we should distinguish between two situations as listed below

$E > 0$ $(s = s' = +1)$	$E < 0$ $(s = s' = -1)$
$\lvert n\rvert > \frac{\lvert B'\rvert}{B}\lvert m\rvert$	$\lvert n\rvert < \frac{\lvert B'\rvert}{B}\lvert m\rvert$

Table 2: Positive and negative energies and their corresponding quantum number configurations.

These energies can be plotted to explicitly illustrate their behavior in terms of different quantities entering in the game, which are given in Figure 4.

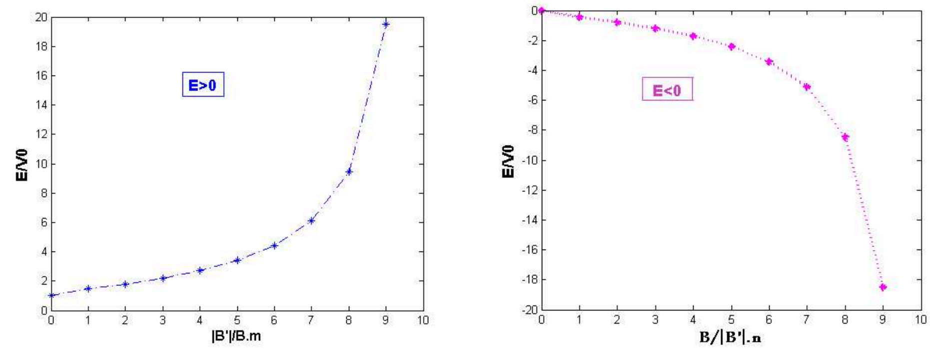

Figure 4: Variation of the ratio $\frac{E}{V_0}$ in terms of $\frac{|B'|}{B}|m|$ for $E > 0$ and $\frac{B}{|B'|}|n|$ for $E < 0$.

3 Two regions in inhomogeneous magnetic field

To treat a concrete example of the present system, we consider a barrier submitted to an inhomogeneous magnetic field. This barrier can be seen as superposition of two regions separated by an interface localized at a fixed point. We study the tunneling effect by evaluating the reflexion and transmission coefficients at interface, which in our case corresponds to the point zero. These will be used to show that the probability condition is exactly one and emphasis what makes difference with respect to without confinement case [19]. To do this task, we follow the same lines as has been done [19] and distinguish between propagation with positive and negative incidences. In both cases we deal with propagation from region I to II, II to III and vice verse.

3.1 Propagation with positive incidence

To proceed, let us first define the eigenspinors for three regions in positive and negative direction of the variable x. In region I, we write

$$\phi_{\mathsf{I},+} = \frac{1}{\sqrt{2}} \begin{pmatrix} -siD_{|n|-1}(x + x_{01}) \\ D_{|n|}(x + x_{01}) \end{pmatrix} e^{ik_y y}, \qquad \phi_{\mathsf{I},-} = \frac{1}{\sqrt{2}} \begin{pmatrix} -siD_{|n|-1}(-x - x_{01}) \\ D_{|n|}(-x - x_{01}) \end{pmatrix} e^{ik_y y}. \tag{33}$$

Similarly, in region II we have

$$\phi_{\mathsf{II},+} = \frac{1}{\sqrt{2}} \begin{pmatrix} -s'iD_{|m|-1}(x + x_{02}) \\ D_{|m|}(x + x_{02}) \end{pmatrix} e^{ik_y y}, \qquad \phi_{\mathsf{II},-} = \frac{1}{\sqrt{2}} \begin{pmatrix} -s'iD_{|m|-1}(-x - x_{02}) \\ D_{|m|}(-x - x_{02}) \end{pmatrix} e^{ik_y y} \tag{34}$$

as well as in region III

$$\phi_{\mathsf{III},+} = \frac{1}{\sqrt{2}} \begin{pmatrix} -siD_{|n|-1}(x + x_{03}) \\ D_{|n|}(x + x_{03}) \end{pmatrix} e^{ik_y y}, \qquad \phi_{\mathsf{III},-} = \frac{1}{\sqrt{2}} \begin{pmatrix} -siD_{|n|-1}(-x - x_{03}) \\ D_{|n|}(-x - x_{03}) \end{pmatrix} e^{ik_y y} \tag{35}$$

where $(\pm)$ refer to the positive and negative propagations, respectively.

We start by analyzing the case of propagation from region I to region II. Indeed, at the interface $x = 0$ (for all y), the continuity of the system gives

$$\phi_{\mathsf{I},+} + r^+_{nm}\phi_{\mathsf{I},-} = t^+_{nm}\phi_{\mathsf{II},+} \tag{36}$$

where r^+_{nm} and t^+_{nm} are reflexion and transmission coefficients, respectively, in positive propagation. From (33) and (34), we obtain

$$\begin{pmatrix} -siD_{|n|-1}(x_{01}) \\ D_{|n|}(x_{01}) \end{pmatrix} + r^+_{nm} \begin{pmatrix} -siD_{|n|-1}(-x_{01}) \\ D_{|n|}(-x_{01}) \end{pmatrix} = t^+_{nm} \begin{pmatrix} -s'iD_{|m|-1}(x_{02}) \\ D_{|m|}(x_{02}) \end{pmatrix}. \tag{37}$$

They can be solved to get the coefficients in terms of some constants, which are magnetic field dependent. They are

$$r^+_{nm}(x_{01}, x_{02}) = (-1)^{|n|} \frac{sA_{\mathsf{I}} - s'B_{\mathsf{I}}}{sA_{\mathsf{I}} + s'B_{\mathsf{I}}} \tag{38}$$

$$t^+_{nm}(x_{01}, x_{02}) = \frac{2sC_{\mathsf{I}}}{sA_{\mathsf{I}} + s'B_{\mathsf{I}}} \tag{39}$$

where we have set

$$\begin{aligned} A_{\mathsf{I}} &= A_{nm}(x_{01}, x_{02}) = D_{|n|-1}(x_{01})D_{|m|}(x_{02}), \\ B_{\mathsf{I}} &= B_{nm}(x_{01}, x_{02}) = D_{|m|-1}(x_{02})D_{|n|}(x_{01}) \\ C_{\mathsf{I}} &= C_n(x_{01}) = D_{|n|-1}(x_{01})D_{|n|}(x_{01}). \end{aligned}$$

On the other hand, considering propagation from region II to region I, the continuity at point zero reads as

$$\phi_{\mathsf{II},+} + r^+_{mn}\phi_{\mathsf{II},-} = t^+_{mn}\phi_{\mathsf{I},+} \tag{40}$$

which implies

$$\begin{pmatrix} s'iD_{|m|-1}(x_{02}) \\ D_{|m|}(x_{02}) \end{pmatrix} + r^+_{mn} \begin{pmatrix} s'D_{|m|-1}(-x_{02}) \\ D_{|m|}(-x_{02}) \end{pmatrix} = t^+_{mn} \begin{pmatrix} sD_{|n|-1}(x_{01}) \\ D_{|n|}(x_{01}) \end{pmatrix}. \tag{41}$$

These lead to the solution

$$r^+_{mn}(x_{01}, x_{02}) = (-1)^{|m|} \frac{s'B_{\mathsf{I}} - sA_{\mathsf{I}}}{sA_{\mathsf{I}} + s'B_{\mathsf{I}}+} \tag{42}$$

$$t^+_{mn}(x_{01}, x_{02}) = \frac{2s'F_{\mathsf{I}}}{sA_{\mathsf{I}} + s'B_{\mathsf{I}}} \tag{43}$$

where F_{I} is

$$F_{\mathsf{I}} = F_m(x_{02}) = D_{|m|-1}(x_{02})D_{|m|}(x_{02}). \tag{44}$$

In similar way, we show that the reflexion and transmission coefficients corresponding to propagation from II to III are given by

$$r^+_{mn}(x_{02}, x_{03}) = (-1)^{|m|} \frac{s'B_{\mathsf{II}} - sA_{\mathsf{II}}}{sA_{\mathsf{II}} + s'B_{\mathsf{II}}} \tag{45}$$

$$t^+_{mn}(x_{02}, x_{03}) = \frac{2s'F_{\mathsf{I}}}{sA_{\mathsf{II}} + s'B_{\mathsf{II}}} \tag{46}$$

where the constants read as

$$A_{\mathsf{II}} = A_{nm}(x_{02}, x_{03}), \qquad B_{\mathsf{II}} = B_{nm}(x_{02}, x_{03}). \tag{47}$$

As far as the propagation from III to II is concerned, we find

$$r^{+}_{nm}(x_{02},x_{03}) = (-1)^{|m|}\frac{sA_{\mathsf{II}}-s'B_{\mathsf{II}}}{sA_{\mathsf{II}}+s'B_{\mathsf{II}}} \tag{48}$$

$$t^{+}_{nm}(x_{02},x_{03}) = \frac{2sC_{\mathsf{II}}}{sA_{\mathsf{II}}+s'B_{\mathsf{II}}} \tag{49}$$

where C_{II} is

$$C_{\mathsf{II}} = C_n(x_{03}). \tag{50}$$

This summarizes our analysis for propagation with positive incidence, which together will be used to discuss different issues and before doing so, we need to analyze negative incidence.

3.2 Propagation with negative incidence

We determine the reflection and transmission coefficients for the propagation with negative incidence, which will be denoted as $r^{-}_{nm/mn}$ and $t^{-}_{nm/mn}$ for the cases of the propagations from I to II, II to III and vice verse. To reply this inquiry, we use the same analysis as before but one should take into account the negative sign of variable.

In doing our task, for region I we write the corresponding eigenspinors as

$$\phi_{\mathsf{I},+} = \frac{1}{\sqrt{2}}\begin{pmatrix} -siD_{|n|-1}(-x-x_{01}) \\ D_{|n|}(-x-x_{01}) \end{pmatrix} e^{ik_y y}, \qquad \phi_{\mathsf{I},-} = \frac{1}{\sqrt{2}}\begin{pmatrix} -siD_{|n|-1}(x+x_{01}) \\ D_{|n|}(x+x_{01}) \end{pmatrix} e^{ik_y y}. \tag{51}$$

For region II, we have

$$\phi_{\mathsf{II},+} = \frac{1}{\sqrt{2}}\begin{pmatrix} -s'iD_{|m|-1}(-x-x_{02}) \\ D_{|m|}(-x-x_{02}) \end{pmatrix} e^{ik_y y}, \qquad \phi_{\mathsf{II},-} = \frac{1}{\sqrt{2}}\begin{pmatrix} -s'iD_{|m|-1}(x+x_{02}) \\ D_{|m|}(x+x_{02}) \end{pmatrix} e^{ik_y y}. \tag{52}$$

In region III, we write

$$\phi_{\mathsf{III},+} = \frac{1}{\sqrt{2}}\begin{pmatrix} -siD_{|n|-1}(-x-x_{03}) \\ D_{|n|}(-x-x_{03}) \end{pmatrix} e^{ik_y y}, \qquad \phi_{\mathsf{III},-} = \frac{1}{\sqrt{2}}\begin{pmatrix} -siD_{|n|-1}(x+x_{03}) \\ D_{|n|}(x+x_{03}) \end{pmatrix} e^{ik_y y}. \tag{53}$$

Now let us treat each case to evaluate reflexion and transmission coefficients. Considering the propagation: $\mathsf{I} \longrightarrow \mathsf{II}$ to obtain

$$\phi_{\mathsf{I},+} + r^{-}_{nm}\phi_{\mathsf{I},-} = t^{-}_{nm}\phi_{\mathsf{II},+} \tag{54}$$

at point zero. Injecting (51) and (52) into (54), one gets

$$r^{-}_{nm}(x_{01},x_{02}) = (-1)^{|n|}\frac{sA_{\mathsf{I}}-s'B_{\mathsf{I}}}{sA_{\mathsf{I}}+s'B_{\mathsf{I}}} \tag{55}$$

$$t^{-}_{nm}(x_{01},x_{02}) = (-1)^{|n|+|m|}\frac{2sC_{\mathsf{I}}}{sA_{\mathsf{I}}+s'B_{\mathsf{I}}}. \tag{56}$$

For $\mathsf{II} \longrightarrow \mathsf{I}$ a similar relation to (54) reads as

$$\phi_{\mathsf{II},+} + r^{-}_{mn}\phi_{\mathsf{II},-} = t^{-}_{mn}\phi_{\mathsf{I},+}. \tag{57}$$

The solutions are given by

$$r^-_{mn}(x_{01},x_{02}) = (-1)^{|m|}\frac{s'B_{\mathsf{I}}-sA_{\mathsf{I}}}{sA_{\mathsf{I}}+s'B_{\mathsf{I}}} \tag{58}$$

$$t^-_{mn}(x_{01},x_{02}) = (-1)^{|n|+|m|}\frac{2s'F_{\mathsf{I}}}{sA_{\mathsf{I}}+s'B_{\mathsf{I}}}. \tag{59}$$

After applying the same technique as before, we show that the propagation: $\mathsf{II} \longrightarrow \mathsf{III}$ gives

$$r^-_{mn}(x_{02},x_{03}) = (-1)^{|m|}\frac{s'B_{\mathsf{II}}-sA_{\mathsf{II}}}{sA_{\mathsf{II}}+s'B_{\mathsf{II}}} \tag{60}$$

$$t^-_{mn}(x_{02},x_{03}) = (-1)^{|n|+|m|}\frac{2s'F_{\mathsf{I}}}{sA_{\mathsf{II}}+s'B_{\mathsf{II}}} \tag{61}$$

and $\mathsf{III} \longrightarrow \mathsf{II}$ leads

$$r^-_{nm}(x_{02},x_{03}) = (-1)^{|n|}\frac{sA_{\mathsf{II}}-s'B_{\mathsf{II}}}{sA_{\mathsf{II}}+s'B_{\mathsf{II}}} \tag{62}$$

$$t^-_{nm}(x_{02},x_{03}) = (-1)^{|n|+|m|}\frac{2sC_{\mathsf{II}}}{sA_{\mathsf{II}}+s'B_{\mathsf{II}}}. \tag{63}$$

By inspecting the forms of different coefficients obtained so far, one can establish a symmetry between them. Indeed, We show the relation

$$\frac{t^{\pm}_{ij}(x_{01},x_{02})}{t^{\mp}_{ij}(x_{01},x_{02})} = -\frac{r^{\pm}_{ij}(x_{01},x_{02})}{r^{\pm}_{ji}(x_{01},x_{02})} = (-1)^{|n|+|m|} \tag{64}$$

where the pair of index is chosen such as $(i \neq j) \in \{n,m\}$. Note that, the same relations are also valid for the couple (x_{02},x_{03}).

3.3 Reflexion and transmission amplitudes

Now let us collect the products of our results by checking their importance. In fact, we discuss the reflexion and transmission amplitudes between regions to emphasis the influence of each parameter on them. For propagation between I and II, we define the reflexion and transmission amplitudes as

$$\rho(x_{01},x_{02}) = r^{\pm}_{ij}(x_{01},x_{02})r^{\mp}_{ij}(x_{01},x_{02}), \qquad \tau(x_{01},x_{02}) = t^{\pm}_{ij}(x_{01},x_{02})t^{\pm}_{ji}(x_{01},x_{02}). \tag{65}$$

After replacing, we end up with

$$\rho(x_{01},x_{02}) = \frac{[sA_{\mathsf{I}}-s'B_{\mathsf{I}}]^2}{[sA_{\mathsf{I}}+s'B_{\mathsf{I}}]^2} \tag{66}$$

$$\tau(x_{01},x_{02}) = \frac{4ss'C_{\mathsf{I}}F_{\mathsf{I}}}{[sA_{\mathsf{I}}+s'B_{\mathsf{I}}]^2} = \frac{4ss'A_{\mathsf{I}}B_{\mathsf{I}}}{[sA_{\mathsf{I}}+s'B_{\mathsf{I}}]^2} \tag{67}$$

where the relation $C_{\mathsf{I}}F_{\mathsf{I}} = A_{\mathsf{I}}B_{\mathsf{I}}$ is satisfied. A straightforward calculation shows that the probability sums to unity, namely

$$\rho(x_{01},x_{02}) + \tau(x_{01},x_{02}) = 1. \tag{68}$$

To stress how the amplitudes behave in terms of different parameters, we give Figure 5. It is clear that, $\rho(x_{01},x_{02})$ and $\tau(x_{01},x_{02})$ change with respect to variation the magnetic field B' for different values of B, m, d and k_y.

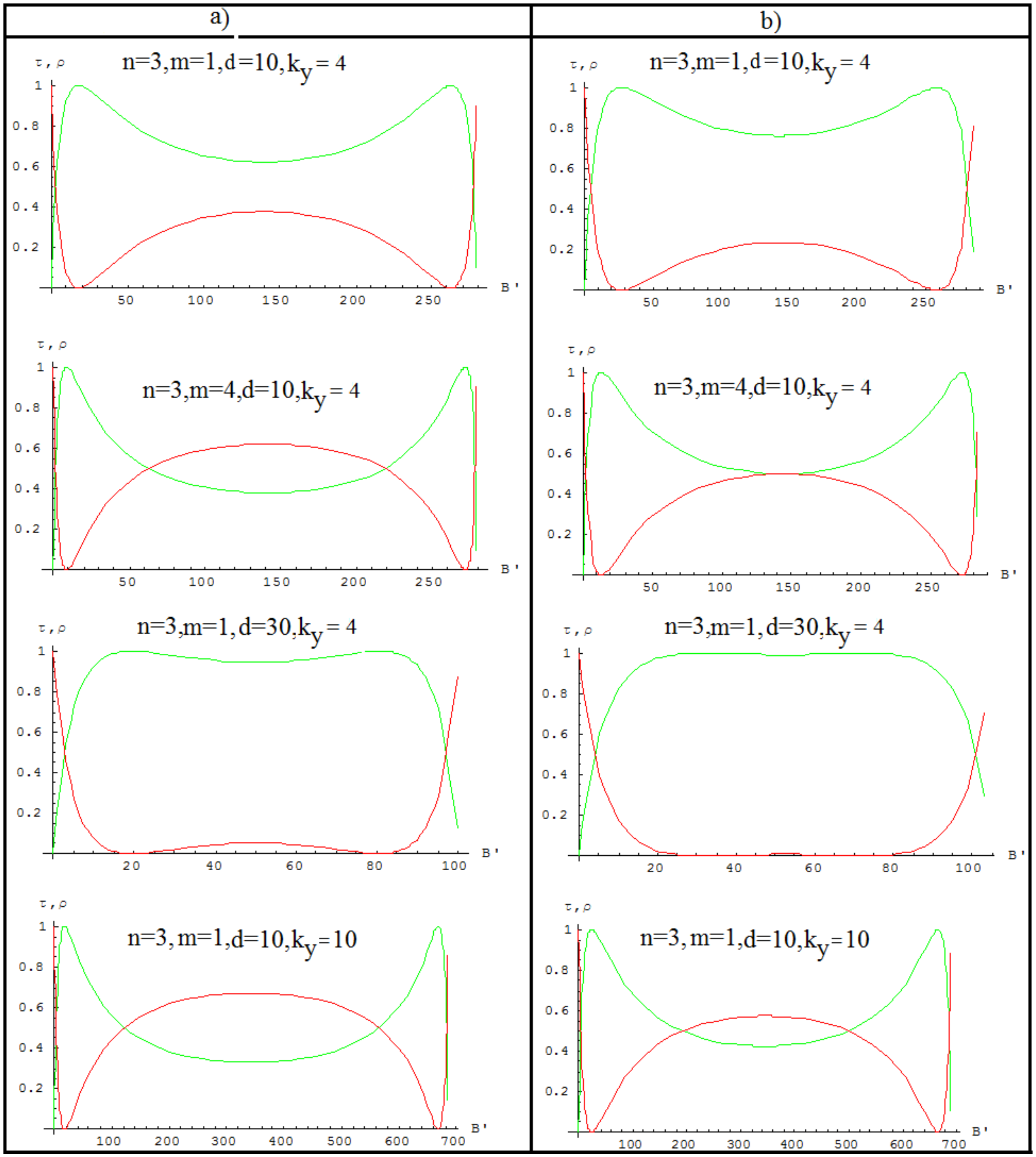

Figure 5: Reflexion $\rho(x_{01}, x_{02})$ (red line) and transmission $\tau(x_{01}, x_{02})$ (green line) coefficients between region I and II for a magnetic barrier of width $2d$ at various magnetic field B' for two cases: a) $B = 10$, b) $B = 15$ and for different values of (m, d, k_y).

It worthwhile to invert the situation by varying B for two values of B' a given configuration of the parameters (m, d, k_y). This summarized as follows

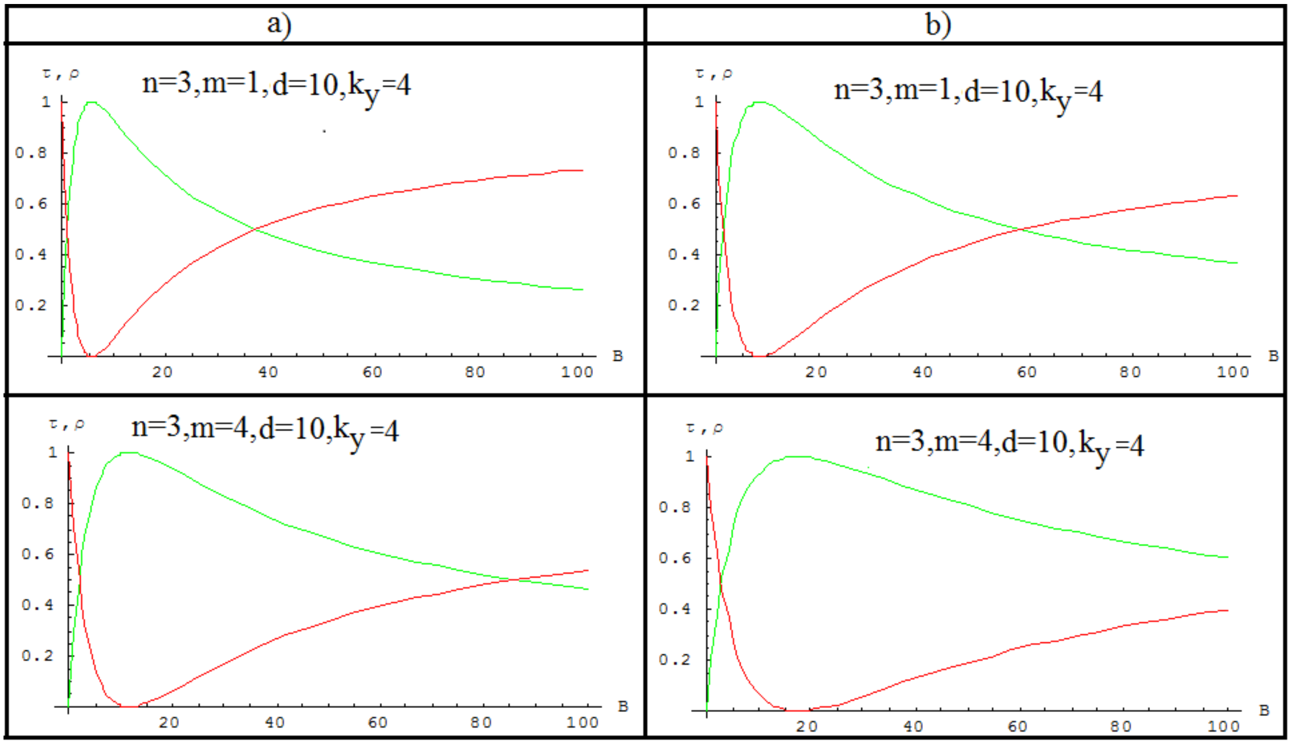

Figure 6: Reflexion $\rho(x_{01}, x_{02})$ (red line) and transmission $\tau(x_{01}, x_{02})$ (green line) coefficients between region I and II for a magnetic barrier of width $2d$ at various magnetic field B for two cases: a) $B' = 10$, b) $B' = 15$ and for different values of (m, d, k_y).

As far as the propagation between II and III is concerned, we use the same definition as above to write the amplitudes

$$\rho(x_{02}, x_{03}) = r_{ij}^{\pm}(x_{02}, x_{03}) r_{ij}^{\mp}(x_{02}, x_{03}), \qquad \tau(x_{02}, x_{03}) = t_{ij}^{\pm}(x_{02}, x_{03}) t_{ji}^{\pm}(x_{02}, x_{03}) \tag{69}$$

which give

$$\rho(x_{02}, x_{03}) = \frac{[sA_{\text{II}} - s'B_{\text{II}}]^2}{[sA_{\text{II}} + s'B_{\text{II}}]^2} \tag{70}$$

$$\tau(x_{02}, x_{03}) = \frac{4ss'C_{\text{II}}F_{\text{I}}}{[sA_{\text{II}} + s'B_{\text{II}}]^2} = \frac{4ss'A_{\text{II}}B_{\text{II}}}{[sA_{\text{II}} + s'B_{\text{II}}]^2} \tag{71}$$

where $C_{\text{II}}F_{\text{I}} = A_{\text{II}}B_{\text{II}}$. Using these to verify

$$\rho(x_{02}, x_{03}) + \tau(x_{02}, x_{03}) = 1. \tag{72}$$

As before we illustrate this result by making different plots, which are given by Figure 7

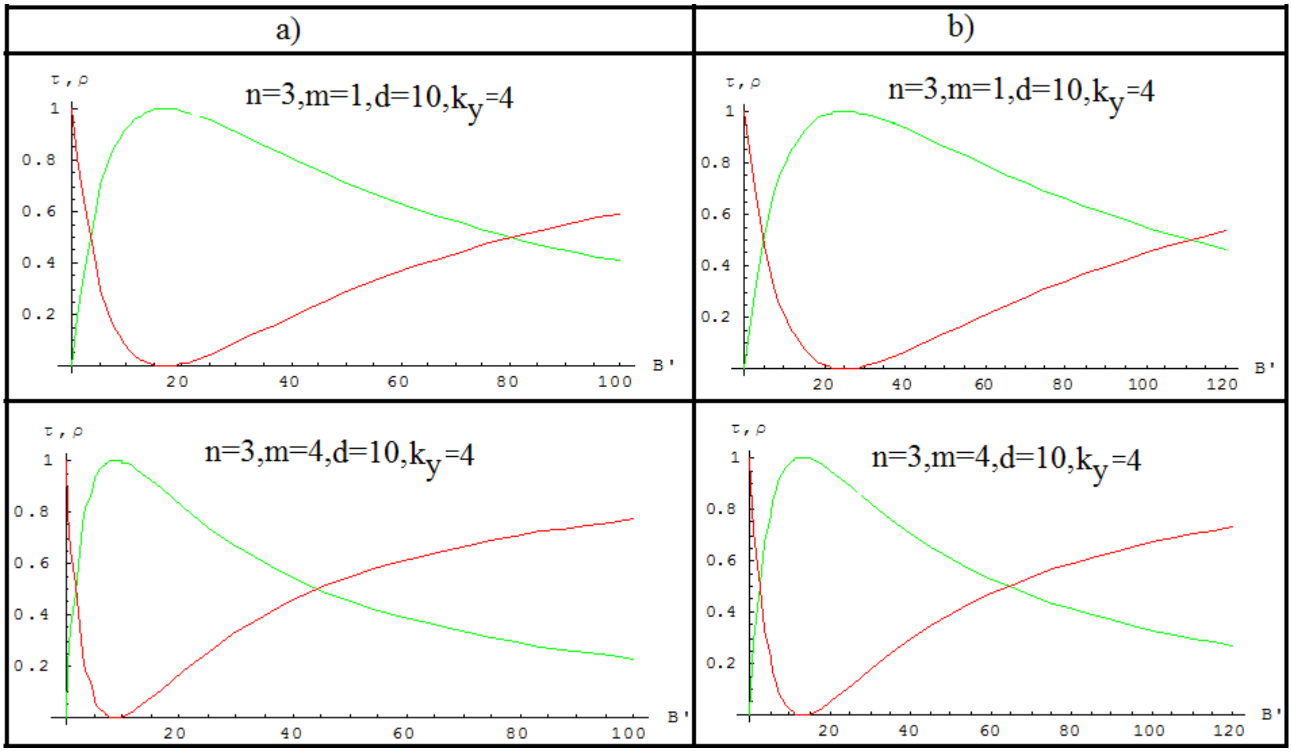

Figure 7: Reflexion $\rho(x_{02}, x_{03})$ (red line) and transmission $\tau(x_{02}, x_{03})$ (green line) coefficients between region II and III for a magnetic barrier of width $2d$ at various magnetic field B' for two cases: a) $B = 10$, b) $B = 15$ and for different values of (m, d, k_y).

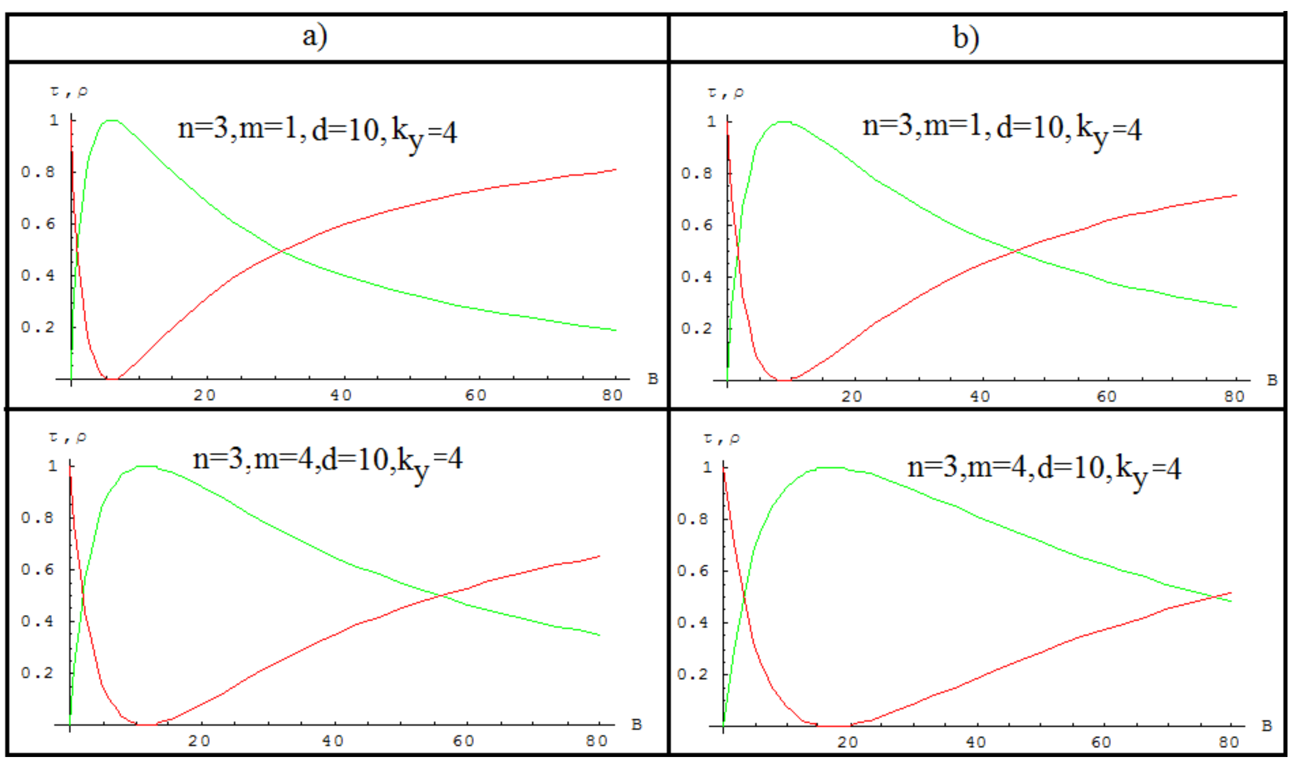

Figure 8: Reflexion $\rho(x_{02}, x_{03})$ (red line) and transmission $\tau(x_{02}, x_{03})$ (green line) coefficients between region II and III for a magnetic barrier of width $2d$ at various magnetic field B for two cases: a) $B' = 10$, b) $B' = 15$ and for different values of (m, d, k_y).

These are among the interesting results derived so far. In fact, it tell us the transmission of barrier in inhomogeneous magnetic fields can not be greater than one, which is analogue to what obtained in one field case and without confinement [19].

Let us present some discussions and derive interesting results those have applications in physics areas. Indeed, similar relations to what obtained above exist also for the photon optics cases. For instance, one can write (68) and (72) when a light beam is reflected and refracted in a diopter between regions I-II and II-III. The first case is characterized by the configuration

- For $n = 0$ $\quad\Longrightarrow\quad \begin{cases} \rho(x_{01}, x_{02}) = 1, & \tau(x_{01}, x_{02}) = 0 \\ \rho(x_{02}, x_{03}) = 1, & \tau(x_{02}, x_{03}) = 0. \end{cases}$

This is an expected result since the transmission $\tau = 1 - \rho$ must be zero in the case where the wave in the n-region enters in the m-region and vice verse. In fact, the interface between tree regions behaves like a mirror where the reflexion is total. The second case is described by

- For $s = s'$ and $n = \pm m$ $\quad\Longrightarrow\quad \begin{cases} \rho(x_{01}, x_{02}) = 0, & \tau(x_{01}, x_{02}) = 1 \\ \rho(x_{02}, x_{03}) = 0, & \tau(x_{02}, x_{03}) = 1 \end{cases}$

which means that the interface between region I-II and II-III behaves like a non-reflective diopter, namely there is a total transmission. Note that, these two cases have interesting interpretation in optics physics.

4 Tree regions in inhomogeneous magnetic fields

We study another case of a physical system composed of a region indexed by the quantum number m of length $2w$ separating two others indexed by the same quantum number n. This will allow us to see how the above results will be changed to the present case and underline what make difference with respect to the former analysis.

4.1 Reflexion and transmission coefficients

The present situation is quiet different from the former one. We use the above tool to write the continuity equation at the points $x = -d$ and $x = d$. Then, we derive the quantities needed to discuss the reflexion and transmission coefficients as well as the corresponding probabilities. This will be done by treating propagation with positive and negative incidences.

We study the positive incidence by considering the geometry that corresponds to the first interface, which is

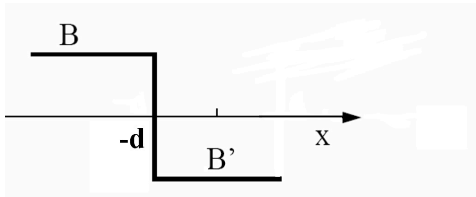

Figure 9: Magnetic field profile between regions I and II.

Using the above spinors to setup the continuity equation at the point $x = -d$. Doing this process to get the relation

$$\phi_{\mathsf{I},+}(-d) + r^+\phi_{\mathsf{I},-}(-d) = \alpha\phi_{\mathsf{II},+}(-d) + \beta\phi_{\mathsf{II},-}(-d) \tag{73}$$

where r^+ is the reflection coefficient for positive incidence, which will be determined together with the parameters α and β. (73) gives

$$sD_{|n|-1}(d_1) + r^+ sD_{|n|-1}(-d_1) = \alpha s' D_{|m|-1}(d_2) + \beta s' D_{|m|-1}(-d_2) \tag{74}$$

$$D_{|n|}(d_1) + r^+ D_{|n|}(-d_1) = \alpha D_{|m|}(d_2) + \beta D_{|m|}(-d_2) \tag{75}$$

with the constants $d_1 = x_{01} - d$ and $d_2 = x_{02} - d$. These can be solved for α and β to obtain

$$\alpha = \frac{sA_{nm}(d_1,d_2) + s'B_{nm}(d_1,d_2) + r^+(-1)^{|n|}\left[s'B_{nm}(d_1,d_2) - sA_{nm}(d_1,d_2)\right]}{2s'F_m(d_2)} \tag{76}$$

$$\beta = \frac{s'B_{nm}(d_1,d_2) - sA_{nm}(d_1,d_2) + r^+(-1)^{|n|}\left[sA_{nm}(d_1,d_2) + s'B_{nm}(d_1,d_2)\right]}{2(-1)^{|m|}s'F_m(d_2)}. \tag{77}$$

In terms of the reflexion and transmission coefficients, we have

$$\alpha = \frac{1}{t^+_{mn}(d_1,d_2)} - r^+ \frac{r^-_{nm}(d_1,d_2)}{t^+_{mn}(d_1,d_2)} \tag{78}$$

$$\beta = (-1)^{|n|+|m|}\left[\frac{r^+}{t^+_{mn}(d_1,d_2)} - \frac{r^-_{nm}(d_1,d_2)}{t^+_{mn}(d_1,d_2)}\right]. \tag{79}$$

To accomplish such analysis we consider the second interface as shown below

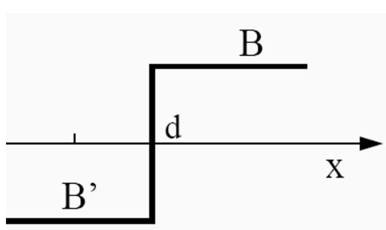

Figure 10: Magnetic field profile between region II and III≡I.

At the point $x = d$, we have

$$\alpha\phi_{\mathsf{II},+}(d) + \beta\phi_{\mathsf{II},-}(d) = t^+\phi_{\mathsf{III},+}(d) \tag{80}$$

where t^+ is transmission coefficient for positive incidence. After replacing, we end up with a system of equations, such as

$$\alpha s' D_{|m|-1}(d_2') + \beta s' D_{|m|-1}(-d_2') = t^+ sD_{|n|-1}(d_3) \tag{81}$$

$$\alpha D_{|m|}(d_2') + \beta D_{|m|}(-d_2') = t^+ D_{|n|}(d_3) \tag{82}$$

with $d_2' = d + x_{02}$ and $d_3 = d + x_{03}$. The solution reads as

$$\begin{aligned}
\alpha &= t^+ \frac{sA_{nm}(d_3, d_2') + s'B_{nm}(d_3, d_2')}{2s'F_m(d_2')} \\
&= \frac{t^+}{t^+_{mn}(d_2', d_3)} \qquad (83)\\
\beta &= t^+(-1)^{|m|} \frac{s'B_{nm}(d_3, d_2') - sA_{nm}(d_3, d_2')}{2s'F_m(d_2')} \\
&= -t^+(-1)^{|n|+|m|} \frac{r^-_{n,m}(d_2', d_3)}{t^+_{mn}(d_2', d_3)} \qquad (84)
\end{aligned}$$

To determine the coefficients for positive incidence we simply use (78-79) and (83-84). Combing all to obtain

$$\begin{aligned}
r^+ &= \frac{r^-_{nm}(d_1, d_2) - r^-_{nm}(d_2', d_3)}{1 - r^-_{nm}(d_1, d_2) r^-_{nm}(d_2', d_3)} \qquad (85)\\
t^+ &= \frac{t^+_{mn}(d_2', d_3)}{t^+_{mn}(d_1, d_2)} \left[\frac{1 - r^-_{nm}(d_1, d_2) r^-_{nm}(d_1, d_2)}{1 - r^-_{nm}(d_1, d_2) r^-_{nm}(d_2', d_3)}\right] \\
&= \frac{t^+_{mn}(d_2', d_3)}{t^+_{mn}(d_1, d_2)} \left[\frac{\tau(d_1, d_2)}{1 - r^-_{nm}(d_1, d_2) r^-_{nm}(d_2', d_3)}\right]. \qquad (86)
\end{aligned}$$

Now let see how the above results will be written by considering the negative incidence case. Indeed, applying the same machinery as before to get

$$\begin{aligned}
r^- &= \frac{r^+_{n,m}(d_1, d_2) - r^+_{n,m}(d_2', d_3)}{1 - r^+_{n,m}(d_1, d_2) r^+_{n,m}(d_2', d_3)} \qquad (87)\\
&= \frac{r^-_{n,m}(d_1, d_2) - r^-_{n,m}(d_2', d_3)}{1 - r^-_{n,m}(d_1, d_2) r^-_{n,m}(d_2', d_3)} \\
t^- &= \frac{t^-_{n,m}(d_2', d_3)}{t^-_{n,m}(d_1, d_2)} \left[\frac{\tau(d_1, d_2)}{1 - r^+_{n,m}(d_1, d_2) r^+_{n,m}(d_2', d_3)}\right] \\
&= \frac{t^-_{n,m}(d_2', d_3)}{t^-_{n,m}(d_1, d_2)} \left[\frac{\tau(d_1, d_2)}{1 - r^-_{n,m}(d_1, d_2) r^-_{n,m}(d_2', d_3)}\right]. \qquad (88)
\end{aligned}$$

Having obtained the above results, we analyze the corresponding probability and give comments. This issue and related matter will be considered in the forthcoming subsection.

4.2 Probability

To characterize the behavior of the present system, we study the incident beam. This can be achieved by calculating the probability of reflexing and transmitting beam. Indeed, let us adopt the definition

$$R = r^+ r^-, \qquad T = t^+ t^-. \qquad (89)$$

After calculation, we find

$$\begin{aligned}
R &= \frac{\rho(d_1, d_2) + \rho(d_2', d_3) - 2r^-_{n,m}(d_1, d_2) r^-_{n,m}(d_2', d_3)}{1 + \rho(d_1, d_2)\rho(d_2', d_3) - 2r^-_{n,m}(d_1, d_2) r^-_{n,m}(d_2', d_3)} \qquad (90)\\
T &= \frac{1 + \rho(d_1, d_2)\rho(d_2', d_3) - \rho(d_1, d_2) - \rho(d_2', d_3)}{1 + \rho(d_1, d_2)\rho(d_2', d_3) - 2r^-_{n,m}(d_1, d_2) r^-_{n,m}(d_2', d_3)}. \qquad (91)
\end{aligned}$$

Combining all to end up with probability

$$R + T = 1. \tag{92}$$

From this, we summarize the following conclusions:

- The probabilities of reflection and transmission sum to unity, as must be the case, since they are the only possible outcomes for a fermion incident on the barrier.
- (90) and (91) yield that under resonance conditions:

  $$|n| = |m|, \qquad s = s'$$

  the barrier becomes transparent, i.e. $T = 1$.
- More significantly, however, the barrier remains always perfectly transparent for $|n| = |m|$.
- $T = 1$ is the feature unique to massless Dirac fermions.
- $T = 1$ is directly related to the Klein paradox in quantum electrodynamics.

5 Introducing gap

In the present study, we consider the confined system in inhomogeneous magnetic field given by the configuration (1) but in the presence of an energy gap t' in the region II. We will show how the above results will be generalized to the gap case.

5.1 Hamiltonian formalism

As far as regions I and III are concerned, the eigenvalues and the eigenfunctions are those given before for case of without t'. However, in region II the Dirac Hamiltonian can be written as

$$H_{\mathsf{II}} = H_{q_y}^{B'} = \upsilon_F \vec{\sigma}\vec{\pi} + V_0 + t'\sigma_z. \tag{93}$$

Clearly, the mass term $t'\sigma_z$ makes difference with respect to the former analysis. In fact, it will play a crucial role and lead to discover interesting results. In terms of matrix, H_{II} takes the form

$$H_{\mathsf{II}} = \upsilon_F \begin{pmatrix} 0 & p_x - ip_y - i\frac{e}{c}A_2(x) \\ p_x + ip_y + i\frac{e}{c}A_2(x) & 0 \end{pmatrix} + \begin{pmatrix} V_0 + t' & 0 \\ 0 & V_0 - t' \end{pmatrix}. \tag{94}$$

For next purpose, we determine the energy spectrum solutions of (94). In doing so, let us fix $\phi_{\mathsf{II}} = \begin{pmatrix} \varphi'_1 \\ \varphi'_2 \end{pmatrix}$ as a spinor of H_{II} in presence of an energy gap t', such as

$$H_{\mathsf{II}} \begin{pmatrix} \varphi'_1 \\ \varphi'_2 \end{pmatrix} = E_{\mathsf{II}} \begin{pmatrix} \varphi'_1 \\ \varphi'_2 \end{pmatrix} \tag{95}$$

which implies two relations

$$-i\hbar\omega'_c D_2 \varphi'_2 = (E_{\mathsf{II}} - V_0 - t')\varphi'_1 \tag{96}$$

$$i\hbar\omega'_c D_2^+ \varphi'_1 = (E_{\mathsf{II}} - V_0 + t')\varphi'_2. \tag{97}$$

They are showing

$$\hbar^2\omega_c'^2 D_2^+ D_2 \varphi_2' = \left[(E_{II} + V_0)^2 - t'^2\right]\varphi_2'. \tag{98}$$

It solution gives the second spinor component as

$$\varphi_2'(x,y) = D_{|m|}\left(x + x_{02}\right)e^{iq_y y}, \qquad m \in \mathbb{Z}. \tag{99}$$

From (98), it is easy to obtain the eigenvalues

$$E_{\mathsf{II},m} = s'\sqrt{\hbar^2\omega_c'^2|m| + t'^2} + V_0. \tag{100}$$

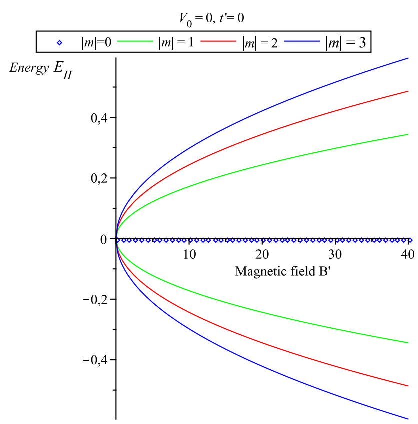

Figure 11: Landau levels E_m in terms of magnetic field B' for different values of m.

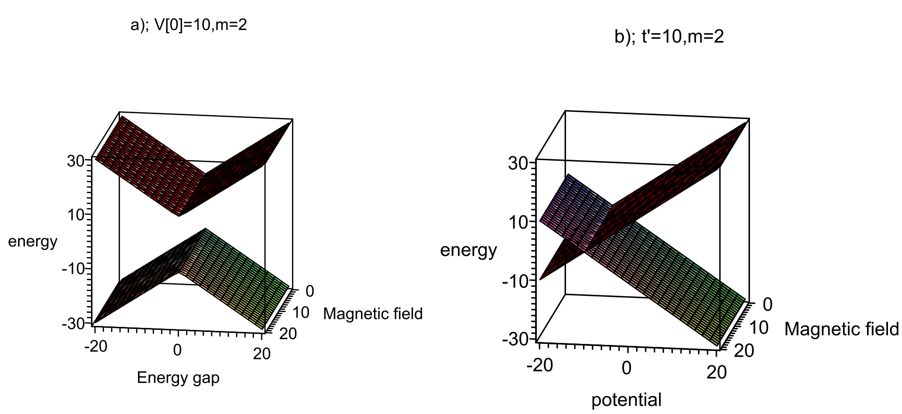

Figure 12: Energy E_m for a magnetic barrier of width $2d$: a) E_m as function of B' and t', b) E_m as function of B' and V_0.

We notice that in the presence of energy gap, there is a gap separating the conduction and valence bands, which is missing in the case where $t' = 0$ (Figure 12b).

To complete the derivation of eigenspinors, we determine the first component φ_1'. Then, from (96) and (97) we obtain

$$\varphi_1'(x,y) = \frac{-i\hbar\omega_c'\sqrt{|m|}}{E_{\mathsf{II}} - V_0 - t'} D_{|m|-1}(x + x_{02})e^{iq_y y}. \tag{101}$$

After normalization the eigenspinors read as

$$\phi_{\mathsf{II},m,q_y}(x,y) = \frac{1}{\sqrt{2}} \begin{pmatrix} -a_m i D_{|m|-1}(x+x_{02}) \\ b_m D_{|m|}(x+x_{02}) \end{pmatrix} e^{iq_y y} \tag{102}$$

where the constants are given by

$$a_m = s' \sqrt{\frac{E_{\mathsf{II}} - V_0 + s't'}{E_{\mathsf{II}}}}, \qquad b_m = \sqrt{\frac{E_{\mathsf{II}} - V_0 - s't'}{E_{\mathsf{II}}}}. \tag{103}$$

As concerning regions I and III, the corresponding eigenspinors $\phi_{\mathsf{I},n,k_y}(x,y,x_{01})$ and $\phi_{\mathsf{III},n,k_y}(x,y,x_{03})$ can be written in compact form as $\phi_{\mathsf{I},n,k_y}(x,y,x_0)$ where

$$x_0 = k_y l_B^2 - \left(1 - \frac{|B'|}{B}\right) x \tag{104}$$

such that $x=-d$ and $x=d$ give $x_0 = x_{01}$ and $x_0 = x_{03}$, respectively.

On the other hand, the energy conservation between regions I and II gives

$$E_{\mathsf{I}} = E_{\mathsf{II}} = E. \tag{105}$$

After replacing, we show that the quantum numbers n and m verify the relation

$$\frac{|n|}{|m|} = \frac{|B'|}{B} \frac{E^2}{(E-V_0)^2 - t'^2}. \tag{106}$$

We have some remarks in order. In region $\mathsf{I}\equiv\mathsf{III}$ we have $V_0 = 0$ and $t' = 0$, thus (106) reduces to

$$\frac{|n|}{|m|} = \frac{|B'|}{B}. \tag{107}$$

However, in region II there two cases:

$$\begin{aligned} (E-V_0)^2 > t'^2 \quad &\Longrightarrow \quad |m| = +m \\ (E-V_0)^2 < t'^2 \quad &\Longrightarrow \quad |m| = -m. \end{aligned} \tag{108}$$

Finally, the analogue of (32) is now given by

$$\frac{E}{V_0} = \frac{\sqrt{|n|}}{\sqrt{|n|} - \frac{s'}{s}\sqrt{\frac{|B'|}{B}|m| + \frac{t'^2}{\hbar^2\omega_c^2}}}. \tag{109}$$

5.2 Reflexion and transmission coefficients in the presence of t'

We will see how the results obtained before can be generalized to the present case. To proceed, we consider two (barrier) and three regions (diode). For barrier, we show that the reflexion and transmission coefficients are

$$\rho'(x_0, x_{02}) = \frac{[sb_m A_{\mathsf{I}} - a_m B_{\mathsf{I}}]^2}{[sb_m A_{\mathsf{I}} + a_m B_{\mathsf{I}}]^2}. \tag{110}$$

$$\begin{aligned} \tau'(x_0, x_{02}) &= \frac{4 s b_m a_m C_{\mathsf{I}} F_{\mathsf{I}}}{[sb_m A_{\mathsf{I}} + a_m B_{\mathsf{I}}]^2} \\ &= \frac{4 s b_m a_m A_{\mathsf{I}} B_{\mathsf{I}}}{[sb_m A_{\mathsf{I}} + a_m B_{\mathsf{I}}]^2} \end{aligned} \tag{111}$$

Clearly, what makes difference with respect to the former results is the appearance of the constant parameters a_m and b_m. These coefficients can be used to verify the probability condition

$$\rho'(x_0, x_{02}) + \tau'(x_0, x_{02}) = 1. \tag{112}$$

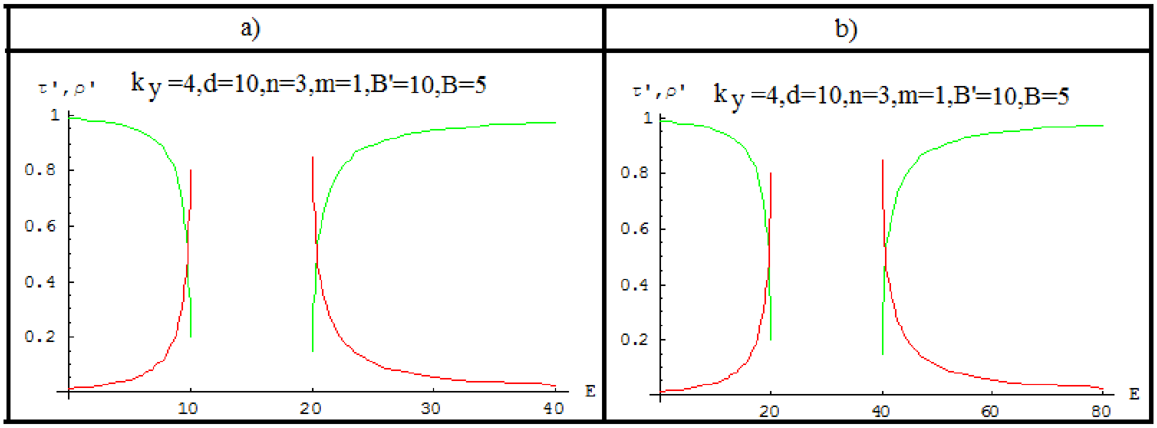

Figure 13: Reflexion $\rho'(x_0, x_{02})$ (red line) and transmission $\tau'(x_0, x_{02})$ (green line) coefficients for a magnetic barrier of width $2d$ at various energy E for two cases: a) $V_0 = 15$, $t' = 5$ and b) $V_0 = 30$, $t' = 10$.

At ($V_0 = 15$, $t' = 5$) and ($V_0 = 30$, $t' = 10$) the transmission and reflexion profile (Figure 13) between regions $\mathsf{I} - \mathsf{II}$ and $\mathsf{II} - \mathsf{III}$ show

- $-t' < E < t'$: $\tau'(x_0, x_{02}) \to 1$ and $\rho'(x_0, x_{02}) \to 0$
- $t' < E < V_0 - t'$: $\tau'(x_0, x_{02})$ decreases and $\rho'(x_0, x_{02})$ increases.
- $V_0 - t' < E < V_0 + t'$: there is no transmission and non reflexion (not allowed states).
- $E > V_0 + t'$: $\tau'(x_0, x_{02}) \to 1$ and $\rho'(x_0, x_{02}) \to 0$.

As far as three regions are concerned, one can inspire from the case without gap to obtain the reflection and transmission amplitudes, such as

$$\textbf{R'} = \frac{\rho'(d_1, d_2) + \rho'(d_3, d_2') - 2r^{+}_{n,m}(d_1, d_2) r^{+}_{n,m}(d_3, d_2')}{1 + \rho'(d_1, d_2)\rho'(d_3, d_2') - 2r^{+}_{n,m}(d_1, d_2) r^{+}_{n,m}(d_3, d_2')} \tag{113}$$

$$\textbf{T'} = \frac{1 + \rho'(d_1, d_2)\rho'(d_2', d_3) - \rho'(d_1, d_2) - \rho'(d_2', d_3)}{1 + \rho'(d_1, d_2)\rho'(d_2', d_3) - 2r^{+}_{n,m}(d_1, d_2) r^{+}_{n,m}(d_2', d_3)}. \tag{114}$$

After a straightforward calculation, we find

$$\textbf{R'+ T'=1}. \tag{115}$$

Note that, for $B = B'$ we discover the results obtained in [19], which shows that our results are more generals.

6 Klein Paradox

We complete the present work by analyzing the Klein paradox for the present system. This can be done by introduce other considerations based on the current-carrying states and study different limiting cases.

6.1 Propagation from region I to region II: $(x = -d)$

We consider the scattering of a Dirac fermion of energy E from an electrostatic step-function potential as shown in Figure 14. This problem is an archetype problem in nonrelativistic quantum mechanics. For relativistic quantum mechanics, we will find that the solution leads to a paradox (Klein paradox) when the potential is strong.

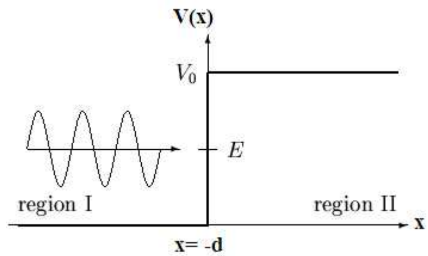

Figure 14: Electrostatic potential idealized with a sharp boundary, with an incident free scalar fermion of energy moving to the right in region I.

According to the previous analysis for two regions, it is easy to note that the solution of the Dirac equation in the region I and II are given by

$$\phi_{x<-d} = \frac{1}{\sqrt{2}} \begin{pmatrix} -siD_{|n|-1}(x+x_{01}) \\ D_{|n|}(x+x_{01}) \end{pmatrix} + \frac{1}{\sqrt{2}} R \begin{pmatrix} -siD_{|n|-1}(-x-x_{01}) \\ D_{|n|}(-x-x_{01}) \end{pmatrix} \tag{116}$$

$$\phi_{x>-d} = \frac{1}{\sqrt{2}} T \begin{pmatrix} -a_m iD_{|m|-1}(x+x_{02}) \\ b_m D_{|m|}(x+x_{02}) \end{pmatrix} \tag{117}$$

where R and T are reflected and transmitted coefficients, respectively. Imposing the boundary condition that ϕ be continuous at $(x = -d)$ gives the relation

$$\begin{pmatrix} sD_{|n|-1}(-d+x_{01}) \\ D_{|n|}(-d+x_{01}) \end{pmatrix} + R \begin{pmatrix} sD_{|n|-1}(d-x_{01}) \\ D_{|n|}(d-x_{01}) \end{pmatrix} = T \begin{pmatrix} a_m D_{|m|-1}(-d+x_{02}) \\ b_m D_{|m|}(-d+x_{02}) \end{pmatrix}. \tag{118}$$

Solving for R and T to obtain

$$R = \frac{sb_m u_1 v_3 - a_m v_1 u_3}{a_m v_2 u_3 - sb_m u_2 v_3} \tag{119}$$

$$T = \frac{s(u_1 v_2 - v_1 u_2)}{a_m v_2 u_3 - sb_m u_2 v_3} \tag{120}$$

where we use the notation

$$\begin{aligned} &u_1 = D_{|n|-1}(-d+x_{01}), \qquad u_2 = D_{|n|-1}(d-x_{01}), \qquad u_3 = D_{|m|-1}(-d+x_{02}) \\ &v_1 = D_{|n|}(-d+x_{01}), \qquad v_2 = D_{|n|}(d-x_{01}), \qquad v_3 = D_{|m|}(-d+x_{02}). \end{aligned} \tag{121}$$

To proceed further, we introduce the current-carrying states. This is based on the current associated to Dirac equation, which is

$$J = ev \sum_i \phi^+ \sigma_i \phi \tag{122}$$

where $i = x, y$. As an immediate application, the incident current is given by

$$J_{\mathsf{I}} = ev \left(\phi_{\mathsf{I}}^+ \sigma_x \phi_{\mathsf{I}} + \phi_{\mathsf{I}}^+ \sigma_y \phi_{\mathsf{I}}\right) = sevu_1 v_1. \tag{123}$$

This can be used to evaluate the final currents to the left and right of the potential boundary, which read as

$$J_{x<-d} = sev\,(u_1 + Ru_2)\,(v_1 + Rv_2) \tag{124}$$

$$J_{x>-d} = \frac{ev}{2}|T|^2 u_3 v_3 \left[i(a_m^+ b_m - a_m b_m^+) + (a_m^+ b_m + a_m b_m^+)\right]. \tag{125}$$

(125) can be split into three parts

$$J_{x>-d} = \begin{cases} -ev|T|^2 a_m b_m u_3 v_3, & V_0 > E + t' \\ -iev|T|^2 a_m b_m u_3 v_3, & E - t' < V_0 < E + t' \\ ev|T|^2 a_m b_m u_3 v_3, & V_0 < E - t' \end{cases} \tag{126}$$

with the condition $a_m b_m > 0$.

Recall that, the reflexion and transmission amplitudes are related to the currents through

$$\mathbf{R} = \frac{J_{\mathsf{I}} - J_{x<-d}}{J_{\mathsf{I}}}, \qquad \mathbf{T} = \frac{J_{x>-d}}{J_{\mathsf{I}}}. \tag{127}$$

After replacing, we end up with

$$\mathbf{R} = \frac{u_1 v_1 \left(a_m v_2 u_3 - s b_m u_2 v_3\right)^2 - a_m b_m u_3 v_3 \left(u_1 v_2 - v_1 u_2\right)^2}{u_1 v_1 \left(a_m v_2 u_3 - s b_m u_2 v_3\right)^2} \tag{128}$$

$$\mathbf{T} = \frac{u_3 v_3 \left[i(a_m^+ b_m - a_m b_m^+) + (a_m^+ b_m + a_m b_m^+)\right] \left(u_1 v_2 - v_1 u_2\right)^2}{2 u_1 v_1 \left(a_m v_2 u_3 - s b_m u_2 v_3\right)^2}. \tag{129}$$

These show that the probability is

$$\mathbf{R} + \mathbf{T} = 1. \tag{130}$$

We can inspect (126) further to derive other results. This can be achieved by considering three interesting cases.

6.2 Limiting cases

In region II there are three distinct cases, depending on the strength of the potential. This is shown by Figure 15:

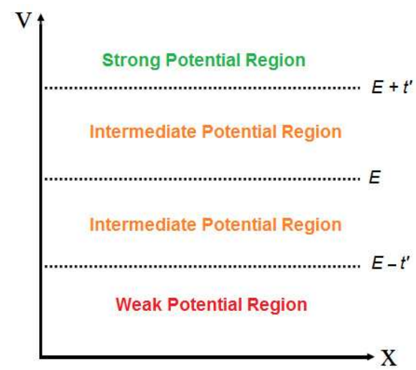

Figure 15: Energy level diagram for a fermion in region II.

Let us analyze each case separately and underline its physical properties. Indeed, in the weak potential that corresponds to $E - V_0 > t'$, we have a restriction on the quantum numbers and parameter constants, such as

$$|m| = +m, \qquad a_m^\dagger = a_m, \qquad b_m^\dagger = b_m.$$

In such case, the reflexion and transmission amplitudes are given by

$$\mathbf{R} = \frac{u_1 v_1 \left(a_m v_2 u_3 - s b_m u_2 v_3\right)^2 - a_m b_m u_3 v_3 \left(u_1 v_2 - v_1 u_2\right)^2}{u_1 v_1 \left(a_m v_2 u_3 - s b_m u_2 v_3\right)^2} \tag{131}$$

$$\mathbf{T} = \frac{a_m b_m u_3 v_3 \left(u_1 v_2 - v_1 u_2\right)^2}{u_1 v_1 \left(a_m v_2 u_3 - s b_m u_2 v_3\right)^2}. \tag{132}$$

They verify the probability condition (130). Thus the incident beam is partly reflected and partly transmitted. This is similar to the result obtained in nonrelativistic quantum mechanics. The last expression shows that the total probability is conserved.

As far as the intermediate potential is concerned, i.e. $|E - V_0| < t'$, different quantities reduce as

$$|m| = -m, \qquad a_m^\dagger = -a_m, \qquad b_m^\dagger = b_m.$$

The corresponding amplitudes are

$$\mathbf{R} \quad = \quad \frac{u_1 v_1 \left(a_m^2 v_2^2 u_3^2 - b_m^2 u_2^2 v_3^2\right)^2 + i a_m b_m u_3 v_3 \left(u_1 v_2 - v_1 u_2\right)^2}{u_1 v_1 \left(a_m^2 v_2^2 u_3^2 - b_m^2 u_2^2 v_3^2\right)^2} \tag{133}$$

$$\mathbf{T} \quad = \quad -\frac{i a_m b_m u_3 v_3 \left(u_1 v_2 - v_1 u_2\right)^2}{u_1 v_1 \left(a_m^2 v_2^2 u_3^2 + b_m^2 u_2^2 v_3^2\right)} \tag{134}$$

where the probabilities sum to unity, as must be the case, since reflection and transmission are the only possible outcomes for a fermion incident on the barrier.

In the strong potential case, i.e. $|E - V_0| > t'$, we have

$$|m| = -m, \qquad a_m^\dagger = -a_m, \qquad b_m^\dagger = -b_m$$

which is showing

$$\mathbf{R} = \frac{u_1 v_1 \left(a_m b_m u_3 v_3 \left(u_1 v_2 - v_1 u_2\right)^2 + a_m v_2 u_3 - s b_m u_2 v_3\right)^2}{u_1 v_1 \left(a_m v_2 u_3 + b_m u_2 v_3\right)^2} > 1 \tag{135}$$

$$\mathbf{T} = -\frac{a_m b_m u_3 v_3 \left(u_1 v_2 - v_1 u_2\right)^2}{u_1 v_1 \left(a_m v_2 u_3 + b_m u_2 v_3\right)^2} < 0. \tag{136}$$

The probability is still conserved, but only at the cost of a negative transmission amplitude and a reflection amplitude which exceeds unity. The strong potential appears to give rise to a paradox. There is no paradox if we consider that in the strong potential case the potential is strong enough to create particle-antiparticle pairs. The antiparticles are attracted by the potential and create a negative charged current moving to the right. This is the origin of the negative transmission amplitude, i.e. (136). The particles, on the other hand, are reflected from the barrier and combined with the incident particle beam (which is completely reflected) leading to a positively charged current, moving to the left and with magnitude greater than that of the incident beam.

7 Conclusion

We considered a system composed of different regions of Dirac fermions in the presence of an inhomogeneous magnetic field and confining potential $V(x)$ in one-direction. The energy spectrum solutions are obtained in terms of different parameters and quantum numbers for each regions. To underline some physical properties of the obtained solutions, we analyzed the energy conservation. This allowed us to establish interesting relations and therefore solve some issues related to reflexion and transmission of the system.

More precisely, by considering our system as as barrier, we derived interesting results. In fact, using the continuity equation at different points we explicitly determined the reflexion and transmission coefficients. These are used to define the corresponding amplitudes and therefore to show that their probabilities sum to unity. Different cases are treated, which concerned total reflecting and transmitting beams where they are interpreted as mirror or diopter systems.

Subsequently, we focussed on three regions of two fixed points d and $-d$. Writing the continuity at each point, we derived different quantities those are needed to characterize the beam of the present system. Indeed, we reached the conclusions that the probabilities of reflection and transmission sum to unity, as must be the case, since they are the only possible outcomes for a fermion incident on the barrier. Furthermore, (90) and (91) yielded that under resonance conditions: $|n| = |m|$ and $s = s'$, the barrier becomes transparent, i.e. $T = 1$. More significantly, however, the barrier remains always perfectly transparent for $|n| = |m|$. This latter is the feature unique to massless Dirac fermions and directly related to the Klein paradox in quantum electrodynamics.

Another interesting cases is analyzed, which concerned introducing a gap. After getting the energy spectrum solutions, we discussed different issues and among them the energy conservation. This allowed us to generalize the former analysis to gap case. As interesting results, we showed that the probabilities of reflecting and transmitting amplitudes sun to unity as well. Requiring that $B = B'$, we recovered the result obtained in [19].

Finally, we discussed the Klein paradox by involving the current-carrying states for different regions. Using their relations to the reflexion and transmission amplitudes, we checked the probability by evaluating different quantities. Moreover, we treated three different limiting cases, which concern week, intermediate and strong potentials. For two last cases, the transmission amplitude is obtained with a negative sign, however when it is added to the reflexion coefficient gives a sum equal unit.

Acknowledgment

The authors are thankful to Dr. El Bouazzaoui Choubabi for fruitful discussions about the tunneling effect in graphene.

References

[1] K.S. Novoselov, A.K. Geim, S.V. Morozov, D. Jiang, M.I. Katsnelson, I.V. Grigorieva, S.V. Dubonos and A.A. Firsov, *Nature* **438** (2005) 197.

[2] Y. Zhang, Y.W. Tan, H.L. Störmer and P. Kim, *Nature* **438** (2005) 201.

[3] C. Berger *et al.*, *Science* **312** (2006) 1191.

[4] N. M. Peres, A. H. Castro Neto and F. Guinea, *Phys. Rev.* **B73** (2006) 241403.

[5] Ö.F. Dayi and A. Jellal, ”A Novel Approach to Confined Dirac Fermions in Graphene”, arXiv:0909.1448.

[6] T.K. Ghosh, A. De Martino, W. Häusler, L. Dell”Anna and R. Egger R, *Phys. Rev.* **B77** (2008) 081404(R), arXiv:0708.1876.

[7] K. Nakada, M. Fujita, G. Dresselhaus, and M.S. Dresselhaus, *Phys. Rev.* **B54** (1996) 17954; E. McCann and V.I. Falko, *J. Phys.: Cond. Matt.* **16** (2004) 2371; N.M.R. Peres, F. Guinea, and A.H. Castro Neto, *Phys. Rev.* **B73** (2006) 125411; ibid. **73** (2006) 241403(R); L. Brey and H.A. Fertig, *Phys. Rev.* **B73** (2006) 235411; D.A. Abanin, P.A. Lee and L.S. Levitov, *Phys. Rev. Lett.* **96** (2006) 176803.

[8] J.C. Meyer, A.K. Geim, M.I. Katsnelson, K.S. Novoselov, T.J. Booth and S. Roth, *Nature* **446** (2007) 60.

[9] J.M. Pereira, V. Mlinar, F.M. Peeters and P. Vasilopoulos, *Phys. Rev.* **B74** (2006) 045424.

[10] N.M.R. Peres, A.H. Castro Neto and F. Guinea, *Phys. Rev.* **B73** (2006) 195411; M.I. Katsnelson, *Eur. Phys. J.* **B57** (2007) 225.

[11] M.Y. Han, B. Ozyilmaz, Y. Zhang and P. Kim, *Phys. Rev. Lett.* **98** (2007) 206805.

[12] P.D. Ye et al., *Phys. Rev. Lett.* **74** (1995) 3013.

[13] For recent work, see M. Cerchez, S. Hugger, T. Heinzel and N. Schulz, *Phys. Rev.* **B75** (2007) 035341, and references therein.

[14] For a review, see S.J. Lee, S. Souma, G. Ihm and K.J. Chang, *Phys. Rep.* **394** (2004) 1.

[15] D. Lawton, A. Nogaret, M.V. Makarenko, O.V. Kibis, S.J. Bending, and M. Henini, *Physica* **E13** (2002) 699; M. Hara, A. Endo, S. Katsumoto and Y. Iye, *Phys. Rev.* **B69** (2004) 153304.

[16] F.M. Peeters and A. Matulis, *Phys. Rev.* **B48** (1993) 15166.

[17] J.E. Muller, *Phys. Rev. Lett.* **68** (1992) 385; S.M. Badalyan and F.M. Peeters, *Phys. Rev. B* **64** (2001) 155303; N. Malkova, I. Gomez and F. Domnguez- Adame, *Phys. Rev.* **B63** (2001) 035317; J. Reijiniers, A. Matulis, K. Chang, F.M. Peeters and P. Vasilopoulos, *Europhys. Lett.* **59** (2002) 749; H.-W. Lee and D.S. Novikov, *Phys. Rev.* **B68** (2003) 155402.

[18] A. De Martino, L. DellAnna and R. Egger, *Phys. Rev. Lett.* **98** (2007) 066802.

[19] E.B. Choubabi, M. El Bouziani and A. Jellal, *Tunneling for Dirac Fermions in Constant Magnetic Field*, arXiv:0906.0097, to appear in Int. J. Geom. Meth. Mod. Phys (2010).

[20] I.S. Gradshteyn and I.M. Ryzhik, "Table of Integrals, Series, and Product" (Academic Press, Inc., 1980).